Granular superconductivity below 5 K in SPI-II pyrolytic graphite

Ana Ballestar, Pablo Esquinazi,* and Winfried Böhlmann
Division of Superconductivity and Magnetism, Institut für Experimentelle Physik II, Universität Leipzig, Linnéstraße 5, D-04103 Leipzig, Germany

(Received 20 October 2014; revised manuscript received 12 December 2014; published 7 January 2015)

We have studied the transport properties of transmission electron microscope (TEM) lamellae obtained from a pyrolytic graphite sample of grade B (SPI-II) with electrical contacts at the edges of the graphene layers. The temperature, magnetic field, input current dependence of the resistance as well as the current-voltage characteristic curves are compatible with the existence of granular superconductivity below 5 K. TEM pictures of the studied lamellae reveal clear differences of the embedded interfaces to those existing in more ordered pyrolytic samples, which appear to be the origin for the relatively lower temperatures at which the granular superconductivity is observed.

DOI: 10.1103/PhysRevB.91.014502 PACS number(s): 74.70.Wz, 74.81.Bd, 74.25.F−

I. INTRODUCTION

Electrical conductivity measurements are an excellent tool to search for superconductivity embedded in nonsuperconducting matrices as in granular superconductors [1,2] or the superconductivity located at certain interfaces formed between materials that are not superconducting [3,4]. In general, it is known that the properties of internal interfaces in solids can be fundamentally different from those of the corresponding bulk materials. In graphite samples, either in highly oriented pyrolytic graphite (HOPG) [5] or in Kish graphite [6], there exist embedded interfaces. These two-dimensional (2D) interfaces represent the border between two graphite crystalline structures with Bernal stacking order but twisted by an angle θ_{twist} [7]. These 2D interfaces were also found at the surfaces of HOPG samples [8–11] as well as in twisted bilayer graphene, where several scanning tunneling microscopy studies with $\theta_{\text{twist}} \lesssim 10^\circ$ [12,13] indicate the existence of van Hove singularities, in agreement with theoretical estimates [14]. We further note that interfaces in pure and doped Bi bicrystals [15,16] can show superconductivity up to $T_c \simeq 21$ K [17], although Bi as bulk is not a superconductor.

Let us clarify to some extent the expected phenomena at the interfaces, following the discussion in Ref. [7]. A rotation with respect to the c axis between single crystalline domains of Bernal graphite can be characterized by a twist angle θ_{twist} that may vary from $\sim 1^\circ$ to $< 60^\circ$ [9]. For twist angles $> 1^\circ$ the graphene layers (or graphite sheets) inside graphite remain unrelaxed giving rise to moiré patterns [8–12,18]. The experimentally confirmed enhancement of the density of states at certain regions of the interface between twisted graphene layers or graphite sheets [8,9,12,13] already suggests a possible enhancement of the probability to have superconductivity, within the mean-field BCS general equations.

An extraordinary result comes out when the twist angle is small enough. In this case the graphene or graphite sheets at the interface can relax their lattices, having perfectly matched regions of certain size $L(\theta_{\text{twist}})$ separated by a network of screw dislocations. For bilayer graphene with slightly twisted layers, these networks can be found in Refs. [13,19,20]. In this case, i.e., at small twist angles, the probability of having high-temperature superconductivity at the interface can be strongly enhanced because in these dislocation regions the dispersion relation at low energies becomes flat [7,20]. Note that a second system of dislocations, in this case edge dislocations, is expected to occur at the boundaries of crystalline Bernal regions when the tilt angle with respect to the c axis $\theta_c \neq 0$. The existence of a flat band in certain regions of the graphite interfaces is of importance because the relationship between the critical temperature T_c and the coupling strength between electrons g changes. Instead of having an exponential dependence, i.e., $T_c \sim T^\star \exp -(1/gN)$ (here $T^\star, N$ are a characteristic temperature range where the Cooper pair coupling applies and the density of states, respectively) it has a linear one, i.e., $T_c \sim g V_{\text{FB}}$ (V_{FB} is the flat band volume) [21–27]. We note that flat bands were found in topological line defects in graphite [28]. Flat bands are believed to be the origin for the relatively high-temperature superconductivity [29] observed at the interfaces of two-layer semiconducting heterostructures [30].

Moreover, interfaces between rhombohedral ($ABCA\ldots$) and Bernal ($ABA\ldots$) stacking order regions have been observed in graphite samples [31,32], which according to theoretical work can be a source for high-temperature superconductivity [22,26]. Calculations indicate that high-temperature superconductivity at the interface can survive throughout the bulk due to the proximity effect between ABC/ABA interfaces where the order parameter is enhanced [26].

Experimental evidence for the existence of granular high-temperature superconductivity in some of those 2D interfaces has been recently published using HOPG samples of high grade [33,34] (see also [35], and references therein). The huge field anisotropy in the magnetoresistance [33] indicates that 2D superconductivity should be located at the interfaces parallel to the graphite sheets.

In this work we are interested in the transport properties of embedded interfaces in HOPG samples of less order, i.e., grade B, because in those samples the 2D interfaces either do not exist or are less clearly defined. As the critical temperature appears to depend on the size or area of the interfaces [34], it is of importance to check whether signs of granular superconductivity can be found in those less ordered samples, especially at lower temperatures in comparison to higher quality samples [33].

*esquin@physik.uni-leipzig.de

II. EXPERIMENTAL DETAILS

For this study we used a HOPG bulk sample of grade II supplied by SPI, namely, SPI-II. This kind of graphite presents a rocking curve width $\sim 0.8^\circ$ (also known as ZYB grade HOPG). Its purity has been thoroughly characterized for several but light elements in Ref. [36] and the results showed that no relevant concentration of foreign elements exists. In order to check for the existence of embedded granular superconductivity in the SPI-II sample we have prepared a transmission electron microscopy (TEM) lamella for transport measurements. To prepare the TEM lamella we used the same procedure as in Refs. [33,34]. The TEM samples have the advantage that through the contact at the graphite sheets and interface edges one strongly enhances the possibility of measuring voltage signals related to those interfaces. The usual method of placing the electrical contacts on the graphite top sheet or at the edges of large samples has the disadvantage that only a small part of the input current goes through the interfaces. Consequently, part of the measured voltage drop is due to the semiconducting graphene layers [37] and/or the contribution of the c-axis resistivity of graphite with the short circuits one has at the grain boundaries. The measured TEM lamella had a length $\times$ width $\times$ thickness equal to $20 \times 5 \times 0.5\ \mu\text{m}^3$ and the current and voltage contacts covered the whole sample width. All the measurements have been performed with the four-probe electrode technique in the conventional configuration.

III. RESULTS AND DISCUSSION

In the inset of Fig. 1 we present a TEM picture of the studied lamella. The white lines crossing the lamella from left to right, approximately parallel to the graphene planes (the c axis is normal to those lines), represent the regions in which the graphene planes are twisted with respect to the gray-color larger regions. By comparison with the TEM pictures taken in HOPG grade A samples, we note that the density of interfaces is much smaller and they are not as sharp and well defined (see Refs. [5,7]).

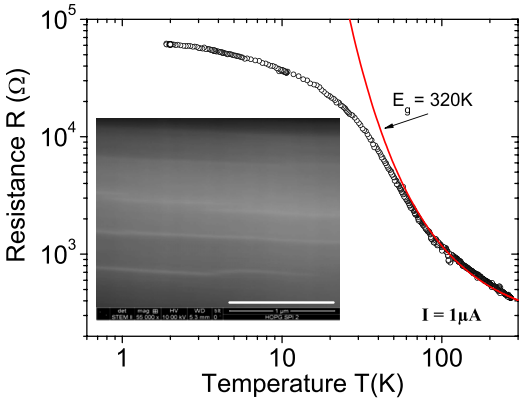

FIG. 1. (Color online) Resistance vs temperature of the TEM lamella at a fixed current of 1 μA. The continuous line follows a simple semiconducting-like exponential function, i.e., $R(T) = 238[\Omega]\exp(E_g/2T)$, where $E_g = 320$ K and T is the temperature. The inset shows a TEM picture of the measured lamella. The scale bar at the bottom right represents 1 μm. The crystalline domains and the borders between them, can be recognized in this TEM picture by the different gray colors. Note that the electron beam is applied parallel to the graphite sheets. The interfaces between regions with a twist angle $\theta_{\text{twist}} > 0$ are located at the borders of regions with uniform gray color. Note that no sharp 2D interfaces can be recognized in this TEM picture, in clear contrast to similar TEM measurements in highly oriented graphite samples [5,33].

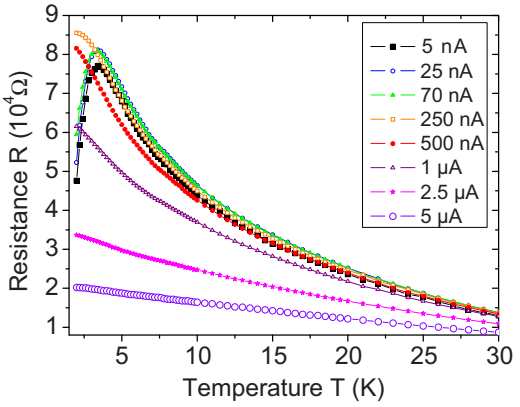

FIG. 2. (Color online) Resistance vs temperature of the TEM lamella at different input currents. For clarity we only show the data below 30 K, the temperature region where the non-Ohmic behavior is clearly observed.

Figure 1 shows the temperature dependence of the resistance measured at a constant input current of 1 μA. Starting from 300 K, the lamella shows a semiconducting-like behavior down to $T \sim 70$ K. Below that temperature the resistance increases slower and tends to saturate at the lowest measured temperatures. To check for a possible non-Ohmic behavior of the resistance, we performed measurements at different input currents. These results are shown in Fig. 2 for temperatures below 30 K. The results at $T \gg 30$ K are current independent (not shown here for clarity). We observe a clear overall increase of the resistance decreasing the input current down to 250 nA. However, for smaller input currents the resistance develops a clear maximum at $T \sim 3$ K (see Fig. 2). The further results we show below indicate that the observed non-Ohmic behavior is related to the existence of superconducting grains embedded in a semiconducting matrix.

The developed maximum in the resistance vs temperature at low input currents already suggests that a coupling between the superconducting grains could exist. An important hint for the existence of granular superconductivity is provided by the magnetic field dependence of the resistance, especially below its maximum. Figure 3(a) shows the resistance vs temperature at different magnetic fields applied normal to the graphene planes. Those measurements have been done at a constant input current of 5 nA. The observed behavior resembles the one seen in the resistance of bulk HOPG samples of similar grade but with contacts at the graphene top layer, i.e., at the sample surface [38,39]. We further note that this behavior is qualitatively identical to the one observed in certain higher grade HOPG samples [40–43], where the metallic-insulating field-driven change is observed up to room temperature. This magnetic field-driven transition, the so-called metal-insulator transition (MIT), was discussed in several papers [39–41] in terms of superconducting-insulator transition because of its analogy to the one observed in MoGe superconducting

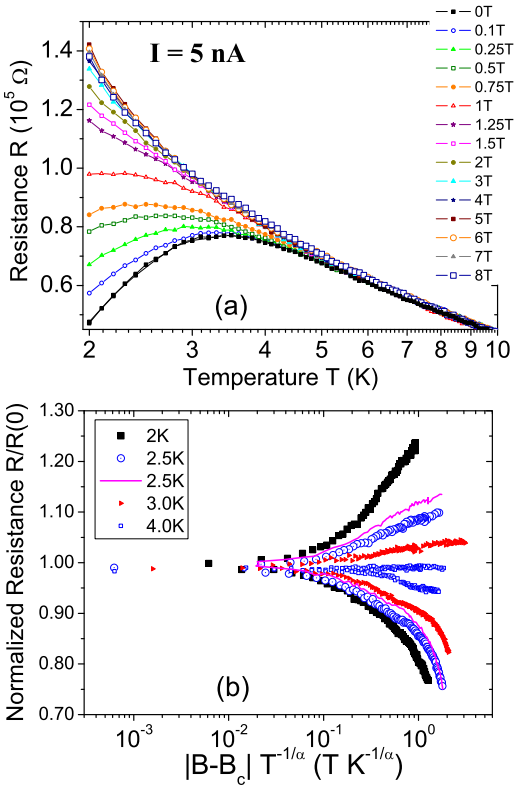

FIG. 3. (Color online) (a) Resistance vs temperature (semilogarithmic scale) at different applied magnetic fields [0 T bottom curve to 8 T upper curve (open squares symbols)] and at an input current of 5 nA. (b) Data obtained from the magnetoresistance measured at 5 nA input current and at different temperatures (not shown here). The x axis is calculated as the absolute field difference $|B - B_c|$ multiplied by the corresponding temperature elevated to the exponent $-1/\alpha$. The curves given by the symbols are obtained at different fixed temperatures and a critical field $B_c = 1$ T and $\alpha = 0.7$. The continuous (red) line at 2.5 K was obtained decreasing the critical field to $B_c = 0.95$ T. The normalization factor in the y axis is $R(|B - B_c| = 0) = 100{,}300\ \Omega$ at all temperatures.

films [44]. The MIT in graphite has also been interpreted using quasiclassical transport equations within the three-dimensional electronic band structure of graphite [45] but with several free magnetic-field-dependent parameters [42,43]. We note, however, that the MIT is observed only if interfaces in the graphite sample exist. The metallicke behavior vanishes for thin enough graphite samples [5,37,46] and obviously the MIT does not exist anymore, indicating that this transition is not intrinsic of the ideal graphite structure.

In bulk HOPG samples the observed MIT shows an interesting scaling that follows to a certain extent the scaling theory for quantum phase transitions in disordered two-dimensional superconductors [47]. In this case the resistance in the critical regime is given by the equation $R(\delta, T) = R_c f(|\delta|, T^{1/\alpha})$ where R_{cr} is the resistance at the transition, $\delta = B - B_c$, B_c is a critical magnetic field, f a scaling function such that $f(0) = 1$, and α a critical exponent. In bulk HOPG samples with MIT excellent scalings have been obtained with $B_c \simeq 0.1 \ldots 0.2$ T and $\alpha = 0.65 \pm 0.05$ [39,41]. With the magnetoresistance measured at 5 nA input current and at different temperatures (not shown here), using $B_c = 1$ T and

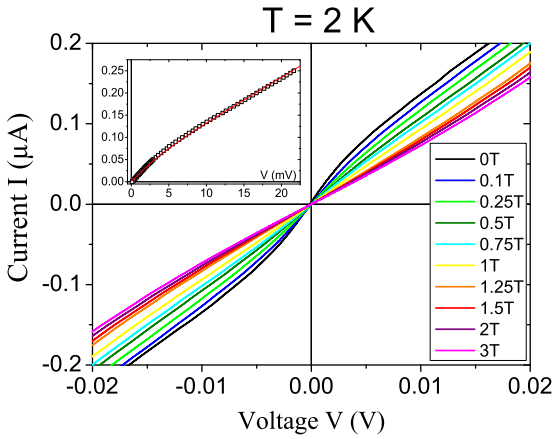

FIG. 4. (Color online) Current-voltage characteristic curves obtained for the TEM lamella at different applied fields at 2 K. The inset shows the curve at zero field with a fit (continuous line) to the differential equation of Ref. [48], using as a free parameter the Josephson critical current $I_c = 82$ nA.

$\alpha = 0.7$ we get the results shown in Fig. 3(b). Although there is a clear similarity to the behavior reported in bulk HOPG samples [39] there is no perfect scaling, i.e., the curves deviate from each other and look less symmetric with respect to the critical $R/R(0) = 1$ line as the temperature increases. The reason for this deviation is the input current dependence of the resistance (see Fig. 2), a dependence that does not exist in bulk HOPG samples mainly due to the distribution of the current along several graphite sheets and interface regions in parallel. Qualitatively speaking the effect of the current with temperature in the scaling behavior of Fig. 3(b) can be partially compensated decreasing the critical field with temperature. As an example, in Fig. 3(b) we show the same data at 2.5 K but with a critical field of 0.95 T instead of 1 T. One recognizes the shift of the upper curve towards the 2 K data and a better symmetry with respect to the critical line. We note further that for the TEM lamella we get a critical exponent α similar to the one obtained in bulk HOPG samples; however, the critical field is one order of magnitude higher [39,41]. This appears to be related to some characteristic size of the superconducting regions, as we will discuss below.

The current-voltage (I-V) characteristic curves at fixed temperature suggest the existence of the Josephson effect between superconducting grains embedded in our lamella. Figure 4 shows the I-V curves obtained at 2 K and at different applied magnetic fields. The curve at zero field as well as the changes observed with field appear compatible with the existence of the Josephson effect. However, even the curve at zero field does not show zero resistance at any current, within experimental resolution. This can be due to, either a finite resistance in series to the embedded Josephson coupled regions, to thermal fluctuation effects, or to both effects simultaneously. The voltage dependence of the differential conductivity $G = dI/dV$ at zero field and different temperatures or at a fixed temperature and different applied fields (see Fig. 5) is compatible with the existence of granular superconductivity. The temperature dependence of the conductivity peak at zero voltage [see Fig. 5(a)] can be tentatively used to estimate by extrapolation the conductivity

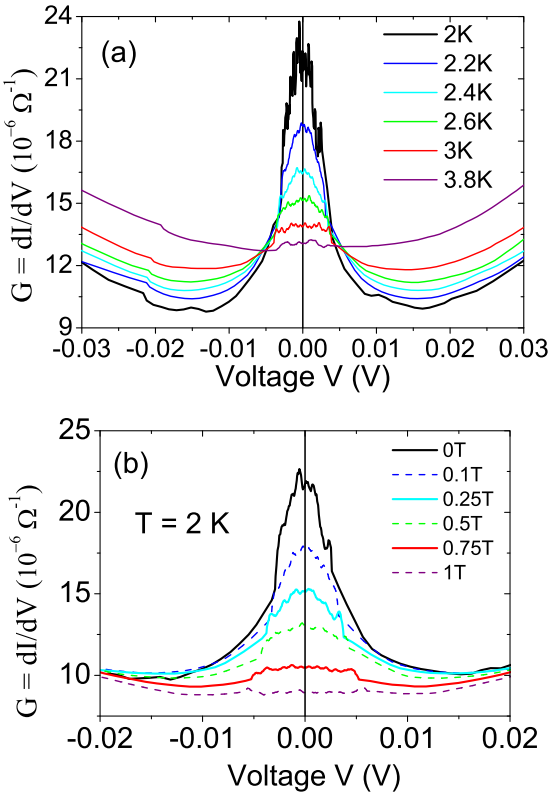

FIG. 5. (Color online) (a) Differential conductivity measured at temperatures between 2 and 3.8 K, i.e., in the temperature range where a finite coupling between the superconducting regions exists. (b) Differential conductivity at 2 K measured at different magnetic fields. The zero field data are the same as in (a) after an average smoothing to remove the noise at low voltages. Above 1 T the nonlinear effect associated with superconducting behavior clearly vanishes.

at zero temperature. In the obviously restricted temperature range the peak in the conductivity follows very well a thermally activated exponential function $G[\Omega^{-1}] \simeq 1.94 \times 10^{-3} \exp(-T/0.38) + 1.3 \times 10^{-5}$, as commonly observed in granular superconductors [1]. The obtained prefactor of the exponential function indicates that the conductivity would grow up to values orders of magnitude larger than the conductivity at high temperatures. Therefore, we assume that the finite conductivity at 2 K is mainly due to thermal fluctuations and not due to an extra resistance in series.

As was done in previous studies [33,34] we account for the thermal fluctuation effects in a Josephson junction [the thermal energy $k_B T$ is larger than the Josephson coupling energy $E_J = (\hbar/2e)I_c$, where I_c is the critical Josephson current] using the differential equation proposed in [48,49]. We fit the measured I-V curves with this model [with the critical current $I_c(T)$ as the only free parameter] and we obtain a very good agreement, as shown in the inset of Fig. 4.

Finally, let us discuss the possible reason for the comparatively low temperature at which the Josephson behavior sets in. We can estimate the size of the Josephson junction using the critical field $B_c \sim 1$ T obtained from the resistance measurements (see Figs. 3 and 4). Following the same arguments as in Ref. [34] we assume that the critical field B_c would produce a single flux quantum in an effective Josephson area. In this case we estimate an area of the order of 45×45 nm^2. This small size and the low critical temperature are compatible with the study on the size dependence of the critical temperature of lamellae with interfaces done in Ref. [34]. Although the origin of this size dependence is not yet completely clarified, we note that this size dependence was already found in conventional superconducting multilayers and thin wires. It has been tentatively interpreted [50,51] as a phenomenon related to weak localization corrections to T_c for 2D superconductors [52]. The key factor to understand the results is the presence of disorder that affects the screening of the Coulomb interaction and therefore the BCS coupling parameter, resulting in an exponential suppression of the critical temperature.

The experimental evidence for the existence of interfaces, the enhancement of the density of states in some of those interfaces regions, as well as the possible existence of anomalously flat bands, provide strong support to recent theories on the importance of flat bands to trigger 2D high-temperature superconductivity. Nevertheless, until all the necessary experimental evidence is obtained, we should not rule out other possibilities that could explain the observed behavior, for example, charge density waves (CDW). We note that evidence for the formation of CDW was found in CaC_6 at $\sim$250 K, a material that becomes superconducting at $T_c = 11.5$ K [53]. Although CDW is antagonist to superconductivity [54], some coexistence with superconductivity has been reported in systems like $NbSe_2$ [55] or $EuBiS_2F$ [56]. The question arises, whether a kind of CDW at the interfaces could be part of the origin of the observed behavior.

IV. CONCLUSION

In summary, the obtained results together with the characteristics of the interfaces observed in TEM pictures for SPI-II HOPG samples, suggest that the superconducting regions at the interfaces are of smaller size than in more ordered HOPG samples, i.e., HOPG grade A. Moreover, the disorder may play a relevant role in lowering the critical temperature where granular superconductivity is observed. The obtained behavior with magnetic field and temperature resembles the MIT found in graphite [39,40,42,43]. Our results indicate that the MIT can be indeed related to superconductivity. The overall results support the existence of superconductivity located at interface regions. Upon the characteristics of the HOPG sample, superconductivity can occur at very high temperatures.

ACKNOWLEDGMENT

This work was partially supported by the Europäischen Sozialfonds (ESF) 100124929.

[1] Y. Shapira and G. Deutscher, Phys. Rev. B **27**, 4463 (1983).

[2] G. Deutscher, *New Superconductors: From Granular to High T_c* (World Scientific, Singapore, 2006).

[3] N. Reyren, S. Thiel, A. D. Caviglia, L. F. Kourkoutis, G. Hammerl, C. Richter, C. W. Schneider, T. Kopp, A.-S. Rüetschia, D. Jaccard *et al.*, Science **317**, 1196 (2007).

[4] A. Gozar, G. Logvenov, L. F. Kourkoutis, A. T. Bollinger, L. A. Giannuzzi, L. A. Muller, and I. Bozovic, Nature (London) **455**, 782 (2008).

[5] J. Barzola-Quiquia, J.-L. Yao, P. Rödiger, K. Schindler, and P. Esquinazi, Phys. Status Solidi A **205**, 2924 (2008).

[6] M. Inagaki, *New Carbons: Control of Structure and Functions* (Elsevier, New York, 2000).

[7] P. Esquinazi, T. T. Heikkilä, Y. V. Lysogoskiy, D. A. Tayurskii, and G. E. Volovik, JETP Lett. **100**, 336 (2014).

[8] M. Kuwabara, D. R. Clarke, and A. A. Smith, Appl. Phys. Lett. **56**, 2396 (1990).

[9] J. H. Warner, M. H. Römmeli, T. Gemming, B. Büchner, and G. A. D. Briggs, Nano Lett. **9**, 102 (2009).

[10] M. Flores, E. Cisternas, J. Correa, and P. Vargas, Chem. Phys. **423**, 49 (2013).

[11] L.-J. Yin, J.-B. Qiao, W.-X. Wang, Z.-D. Chu, K. F. Zhang, R.-F. Dou, C. L. Gao, J.-F. Jia, J.-C. Nie, and L. He, Phys. Rev. B **89**, 205410 (2014).

[12] I. Brihuega, P. Mallet, H. González-Herrero, G. Trambly de Laissardière, M. M. Ugeda, L. Magaud, J. M. Gómez-Rodríguez, F. Ynduráin, and J.-Y. Veuillen, Phys. Rev. Lett. **109**, 196802 (2012).

[13] X. Gong and E. J. Mele, Phys. Rev. B **89**, 121415 (2014).

[14] R. Bistritzer and A. MacDonald, Proc. Natl. Acad. Sci. USA **108**, 12233 (2011).

[15] F. M. Muntyanu, A. Gilewski, K. Nenkov, J. Warchulska, and A. J. Zaleski, Phys. Rev. B **73**, 132507 (2006).

[16] F. M. Muntyanu, A. Gilewski, K. Nenkov, A. J. Zaleski, and V. Chistol, Phys. Rev. B **76**, 014532 (2007).

[17] F. Muntyanua, A. Gilewski, K. Nenkov, A. Zaleski, and V. Chistol, Solid State Commun. **147**, 183 (2008).

[18] J. Biscaras, N. Bergeal, S. Hurand, C. Grossetête, A. Rastogi, R. C. Budhani, D. LeBoeuf, C. Proust, and J. Lesueur, Phys. Rev. Lett. **108**, 247004 (2012).

[19] J. S. Alden, A. W. Tsen, P. Y. Huang, R. Hovden, L. Brown, J. Park, D. A. Muller, and P. L. McEuen, Proc. Natl. Acad. Sci. USA **110**, 11256 (2013).

[20] P. San-Jose and E. Prada, Phys. Rev. B **88**, 121408(R) (2013).

[21] T. Heikkilä, N. B. Kopnin, and G. Volovik, JETP Lett. **94**, 233 (2011).

[22] N. B. Kopnin, M. Ijäs, A. Harju, and T. T. Heikkilä, Phys. Rev. B **87**, 140503 (2013).

[23] V. Khodel and V. Shaginyan, JETP Lett. **51**, 553 (1990).

[24] N. B. Kopnin, T. T. Heikkilä, and G. E. Volovik, Phys. Rev. B **83**, 220503 (2011).

[25] G. E. Volovik, J. Supercond. Novel Magn. **26**, 2887 (2013).

[26] W. A. Muñoz, L. Covaci, and F. M. Peeters, Phys. Rev. B **87**, 134509 (2013).

[27] G. E. Volovik, arXiv:1409.3944.

[28] L. Feng, X. Lin, L. Meng, J.-C. Nie, J. Ni, and L. He, Appl. Phys. Lett. **101**, 113113 (2012).

[29] E. Tang and L. Fu, Nat. Phys. **10**, 964 (2014).

[30] N. Y. Fogel, E. I. Buchstab, Y. V. Bomze, O. I. Yuzephovich, M. Y. Mikhailov, A. Y. Sipatov, E. A. Pashitskii, R. I. Shekhter, and M. Jonson, Phys. Rev. B **73**, 161306 (2006).

[31] Q. Lin, T. Li, Z. Liu, Y. Song, L. He, Z. Hu, Q. Guo, and H. Ye, Carbon **50**, 2369 (2012).

[32] S. Hattendorf, A. Georgi, M. Liebmann, and M. Morgenstern, Surf. Sci. **610**, 53 (2013).

[33] A. Ballestar, J. Barzola-Quiquia, T. Scheike, and P. Esquinazi, New J. Phys. **15**, 023024 (2013).

[34] A. Ballestar, T. T. Heikkilä, and P. Esquinazi, Supercond. Sci. Technol. **27**, 115014 (2014).

[35] P. Esquinazi, Papers Phys. **5**, 050007 (2013).

[36] D. Spemann, P. Esquinazi, A. Setzer, and W. Böhlmann, AIP Adv. **4**, 107142 (2014).

[37] N. García, P. Esquinazi, J. Barzola-Quiquia, and S. Dusari, New J. Phys. **14**, 053015 (2012).

[38] Y. Kopelevich, V. V. Lemanov, S. Moehlecke, and J. H. S. Torres, Fiz. Tverd. Tela **41**, 2135 (1999) [Phys. Solid State **41**, 1959 (1999)].

[39] H. Kempa, Y. Kopelevich, F. Mrowka, A. Setzer, J. H. S. Torres, R. Höhne, and P. Esquinazi, Solid State Commun. **115**, 539 (2000).

[40] Y. Kopelevich, J. H. S. Torres, R. R. da Silva, F. Mrowka, H. Kempa, and P. Esquinazi, Phys. Rev. Lett. **90**, 156402 (2003).

[41] Y. Kopelevich, P. Esquinazi, J. H. S. Torres, R. R. da Silva, and H. Kempa, *Graphite as a Highly Correlated Electron Liquid*, edited by B. Kramer, Advances in Solid State Physics Vol. 43 (Springer-Verlag, Berlin, 2003), pp. 207–222.

[42] T. Tokumoto, E. Jobiliong, E. Choi, Y. Oshima, and J. Brooks, Solid State Commun. **129**, 599 (2004).

[43] X. Du, S.-W. Tsai, D. L. Maslov, and A. F. Hebard, Phys. Rev. Lett. **94**, 166601 (2005).

[44] N. Mason and A. Kapitulnik, Phys. Rev. Lett. **82**, 5341 (1999).

[45] J. W. McClure, IBM J. Res. Dev. **8**, 255 (1964).

[46] R. Vansweevelt, V. Mortet, J. DHaen, B. Ruttens, C. V. Haesendonck, B. Partoens, F. M. Peeters, and P. Wagner, Phys. Status Solidi A **208**, 1252 (2011).

[47] M. P. A. Fisher, Phys. Rev. Lett. **65**, 923 (1990).

[48] V. Ambegaokar and B. I. Halperin, Phys. Rev. Lett. **22**, 1364 (1969).

[49] Y. M. Ivanchenko and L. A. Zil'berman, Zh. Eksp. Teor. Fiz. **55**, 2395 (1968) [Sov. Phys. JETP **28**, 1272 (1969)]. See also *idem*, Zh. Eksp. Teor. Fiz. Pis. Red. **8**, 189 (1968) [JETP Lett. **8**, 113 (1968)].

[50] J. Guimpel, M. E. de la Cruz, F. de la Cruz, H. J. Fink, O. Laborde, and J. C. Villegier, J. Low Temp. Phys. **63**, 151 (1986).

[51] Y. Oreg and A. M. Finkel'stein, Phys. Rev. Lett. **83**, 191 (1999).

[52] H. Fukuyama, Physica B+C **126**, 306 (1984); see also H. Ebisawa, H. Fukuyama, and S. Maekawa, J. Phys. Soc. Jpn. **54**, 2257 (1985).

[53] K. C. Rahnejat, C. A. Howard, N. E. Shuttleworth, S. R. Schofield, K. Iwaya, C. F. Hirjibehedin, C. Renner, G. Aeppli, and M. Ellerby, Nat. Commun. **2**, 558 (2011).

[54] A. M. Gabovich and A. I. Voitenko, Low Temp. Phys. **39**, 232 (2013).

[55] A. Soumyanarayanan, M. M. Yee, Y. He, J. van Wezel, D. J. Rahn, K. Rossnagel, E. W. Hudson, M. R. Norman, and J. E. Hoffman, Proc. Natl. Acad. Sci. **110**, 1623 (2013).

[56] H.-F. Zhai, Z.-T. Tang, H. Jiang, K. Xu, K. Zhang, P. Zhang, J.-K. Bao, Y.-L. Sun, W.-H. Jiao, I. Nowik *et al.*, Phys. Rev. B **90**, 064518 (2014).